

文章编号:1671-6833(2022)04-0001-07

电驱动机械臂的自抗扰鲁棒哈密顿跟踪控制

曾庆山, 周亚帅, 陶长春, 刘艳红

(郑州大学 电气工程学院, 河南 郑州 450001)

摘要: 针对永磁同步电机驱动机械臂系统的位置跟踪问题提出了自抗扰控制与哈密顿控制相结合的鲁棒控制策略。首先,建立了考虑不确定性的电气子系统和机械子系统模型,依据独立关节控制思想将模型转化为单电机驱动单关节的端口哈密顿结构;其次,设计级联扩张状态观测器估计机械子系统的总扰动,设计控制律实现期望位置鲁棒跟踪的同时简单有效地获取到期望的 q 轴电流 I_{qi}^* ;最后,基于系统哈密顿结构设计互联和阻尼配置哈密顿控制器与 H_∞ 控制器相结合的鲁棒哈密顿控制器,实现对电流的高精度鲁棒跟踪,并通过适当改进 H_∞ 的引入时机改善了初始控制输入过大的问题。与电驱动机械臂系统无模型自抗扰控制的仿真对比结果验证了所提控制方案的有效性,级联 ESO 与传统 ESO 相比,关节位置跟踪精度提升了 0.003 rad,改进的鲁棒哈密顿控制器与哈密顿控制器相比关节位置跟踪精度提升了 0.005 rad,电流跟踪精度显著提升,改进 H_∞ 的引入时机使初始控制输入显著降低。

关键词: 电驱动机械臂; 跟踪控制; 端口哈密顿系统; 自抗扰控制; 鲁棒控制

中图分类号: TP391.4

文献标志码: A

doi:10.13705/j.issn.1671-6833.2022.04.017

0 引言

高精度的关节位置跟踪是机器人领域的基本需求。为了降低位置跟踪控制器的设计难度,执行器的动态模型往往被忽略。然而忽略掉执行器的动态,闭环系统的性能可能会降低,甚至不稳定^[1]。永磁同步电机(permanent magnet synchronous motors, PMSM)具有转矩体积比大、精度高、调速范围宽等优点^[2-4],是机器人系统的常用执行装置。

电驱动机械臂的跟踪控制包括位置跟踪^[5-6]以及电流跟踪^[7]。徐旭等^[8]设计了位置协调控制器和反步法电流控制器,但没有考虑系统不确定性的影响。Xue 等^[9]设计了改进的模糊反步法位置控制器,但是没有考虑电动机动态的参数变化及其扰动。Khorashadizadeh 等^[10]设计了自适应模糊控制器对总的不确定性进行估计和补偿。Keighobadi 等^[11]和 Saleki 等^[12]针对永磁直流电机驱动机械臂系统的轨迹跟踪,利用机械臂是电机的负载这个事实,把机械臂动态转换到电气动

态,分别设计了自适应鲁棒反步法控制器和无模型自抗扰控制器(active disturbance rejection control, ADRC)。

Ortega 等^[13]提出的互联和阻尼配置(interconnections and damping assignment, IDA)由于具有物理意义明确、易于设计的优点,被广泛用于哈密顿系统控制设计,此外利用了哈密顿系统的结构和能量特性,便于进行闭环系统稳定性分析和 H_∞ 控制器设计^[3]。但是该方法依赖于系统模型,所设计的鲁棒控制器具有一定的保守性。Han^[14]提出的 ADRC 对模型的依赖程度低,可同时提高系统的抗扰性能和跟踪控制精度,得以广泛应用。Han 等^[7]和金宁治等^[15]将 ADRC 与 IDA 相结合,取得了很好的控制效果。但由于控制增益的不确定性也归入到总扰动中会导致总扰动的估计出现误差,从而使 ADRC 控制性能降低^[16],对此一些学者在 ADRC 中引入滑模控制^[17]和改进扩张状态观测器结构^[18](extended state observer, ESO)处理剩余的扰动观测误差。

本文针对带有不确定性的 PMSM 驱动刚性

收稿日期:2021-11-22; 修订日期:2022-02-23

基金项目:国家自然科学基金资助项目(62003309, 62103376); 科技部重点研发计划项目(2020YFB131370)

作者简介:曾庆山(1963—),男,湖北武汉人,郑州大学教授,博士,主要从事智能控制理论、复杂系统的建模与控制、分数阶微分控制等研究,E-mail:qszeng@126.com。

通信作者:刘艳红(1970—),女,河南郑州人,郑州大学教授,博士,博士生导师,主要从事机器人建模与控制和智能人机交互的研究,E-mail:liuyh@zzu.edu.cn。

机械臂的位置跟踪问题,首先,建立带有不确定性的电驱动机械臂的机械和电气数学模型,依据独立关节控制思想,将关节间的耦合项看作干扰,将 n 个自由度的机械臂系统视为 n 个独立系统,建立单电机驱动单关节的端口哈密顿结构;其次,设计级联 ESO 位置控制器,简单有效地获取到了期望的 q 轴电流 I_{qi}^* ;最后,设计 IDA 与 H_∞ 相结合的鲁棒 IDA 控制器实现关节末端位置跟踪和电流跟踪,并改进了 H_∞ 控制引入的时机,改善了初始控制输入大的问题。

1 机器人系统动态模型

考虑 n 个PMSM 驱动 n 个关节的机器人系统,假定机械系统是刚性的,每一个连杆由一个 PMSM 通过齿轮驱动。带有不确定性的第 i 个关节和电机的机械方程可描述为^[11,13,19]

$$(J_i + \Delta J_i) \ddot{\theta}_i + (B_i + \Delta B_i) \dot{\theta}_i + k_i \tau_{Li} = \tau_{Mi}; \quad (1)$$

$$(M_{ii} + \Delta M_{ii}) \ddot{Q}_i + (C_{ii} + \Delta C_{ii}) \dot{Q}_i + G_i + \Delta G_i + \sum_{\substack{j=1 \\ j \neq i}}^n [(M_{ij} + \Delta M_{ij}) \ddot{Q}_j + (C_{ij} + \Delta C_{ij}) \dot{Q}_j] + F_i = \tau_{Li} + \tau_{exti}. \quad (2)$$

式中: Q_i, θ_i 分别为第 i 个关节和电机转子的位置,rad; $M_{ij}, C_{ij}, G_i, F_i, \tau_{Li}, \tau_{Mi}, \tau_{exti}$ 分别为惯性矩阵元素、哥式力和离心力矩阵元素、重力矩阵元素、关节摩擦力矩矩阵元素、负载转矩矩阵元素、电磁转矩矩阵元素、外部扰动向量的元素; J_i, B_i 分别为电机的惯性矩阵的元素和阻尼矩阵的元素; k_i 为齿轮减速比系数。

假定传动装置是刚性的,没有间隙,转子位置 θ_i 和关节位置 Q_i 存在线性关系 $Q_i = k_i \theta_i$, 将式(2)代入到式(1)得

$$\bar{M}_{ii} \ddot{Q}_i + \bar{C}_{ii} \dot{Q}_i + \tau'_{Li} = \tau_{Mi} + \tau_{disi}. \quad (3)$$

式中: $\bar{M}_{ii} = J_i k_i^{-1} + k_i M_{ii}$; $\bar{C}_{ii} = B_i k_i^{-1} + k_i C_{ii}$; $\tau'_{Li} = k_i G_i + k_i \sum_{\substack{j=1 \\ j \neq i}}^n (M_{ij} \ddot{Q}_j + C_{ij} \dot{Q}_j)$; τ_{disi} 为机械子系统参数变化、外部扰动、摩擦、关节耦合混在一起的总扰动,可由式(4)求得

$$\tau_{disi} = -\Delta J_i k_i^{-1} \ddot{Q}_i - \Delta B_i k_i^{-1} \dot{Q}_i - k_i \Delta M_{ii} \ddot{Q}_i - k_i \Delta C_{ii} \dot{Q}_i - k_i F_i + k_i \tau_{exti} - k_i \sum_{\substack{j=1 \\ j \neq i}}^n (\Delta M_{ij} \ddot{Q}_j + \Delta C_{ij} \dot{Q}_j). \quad (4)$$

第 i 个PMSM 的电磁转矩和电气动态为^[2-4,7]

$$\left\{ \begin{array}{l} \tau_{Mi} = n_p(\phi_i + \Delta\phi_i)I_{qi} + n_p(L_{di} + \Delta L_{di} - L_{qi} - \Delta L_{qi})I_{di}I_{qi}; \\ (L_{di} + \Delta L_{di}) \frac{dI_{di}}{dt} = -(R_i + \Delta R_i)I_{di} + n_p(L_{qi} + \Delta L_{qi})I_{qi}k_i^{-1}\dot{Q}_i + u_{di}; \\ (L_{qi} + \Delta L_{qi}) \frac{dI_{qi}}{dt} = -(R_i + \Delta R_i)I_{qi} - n_p(L_{di} + \Delta L_{di})I_{di}k_i^{-1}\dot{Q}_i - n_p(\phi_i + \Delta\phi_i)k_i^{-1}\dot{Q}_i + u_{qi}. \end{array} \right. \quad (5)$$

式中: L_{di}, L_{qi} 分别为 d, q 轴标称电感系数,H; R_i 为标称定子电阻,Ω; n_p 为磁极对数; $\phi_i = \sqrt{1.5}\phi_{fi}$, ϕ_{fi} 为标称永磁体磁链,Wb; I_{di}, I_{qi} 分别为 d, q 轴定子电流,A; u_{di}, u_{qi} 为 d, q 轴定子电压,V。

把式(3)代入到式(5)的电磁转矩方程中,并令 $f_{mi} = n_p \Delta\phi_i I_{qi} + n_p(\Delta L_{di} - \Delta L_{qi})I_{di}I_{qi}$, $f_{di} = \Delta R_i I_{di} - n_p \Delta L_{qi} I_{qi} k_i^{-1} \dot{Q}_i + \Delta L_{di} \frac{dI_{di}}{dt}$, $f_{qi} = \Delta R_i I_{qi} + n_p(\Delta L_{di} I_{di} + \Delta\phi_i)k_i^{-1}\dot{Q}_i + \Delta L_{qi} \frac{dI_{qi}}{dt}$, 则式(5)可转换为

$$\left\{ \begin{array}{l} L_{di} \frac{dI_{di}}{dt} = -R_i I_{di} + n_p L_{qi} I_{qi} k_i^{-1} \dot{Q}_i + u_{di} - f_{di}; \\ L_{qi} \frac{dI_{qi}}{dt} = -R_i I_{qi} - n_p L_{di} I_{di} k_i^{-1} \dot{Q}_i - n_p \phi_i k_i^{-1} \dot{Q}_i + u_{qi} - f_{qi}; \\ k_i^{-1} \bar{M}_{ii} \ddot{Q}_i = n_p \phi_i k_i^{-1} I_{qi} + n_p k_i^{-1} (L_{di} - L_{qi}) I_{di} I_{qi} - k_i^{-1} \bar{C}_{ii} \dot{Q}_i - k_i^{-1} \tau'_{Li} + k_i^{-1} f_{mi} + k_i^{-1} \tau_{disi}. \end{array} \right. \quad (6)$$

式(6)的状态向量、输入向量、输出向量和扰动向量定义为

$$\left\{ \begin{array}{l} \mathbf{x}_i = [L_{di} I_{di} \quad L_{qi} I_{qi} \quad Q_i \quad k_i^{-1} \bar{M}_{ii} \dot{Q}_i]^T; \\ \mathbf{y}_i = [I_{di} \quad I_{qi}]^T; \\ \mathbf{u}_i = [u_{di} \quad u_{qi}]^T; \\ \mathbf{f}_i = [-f_{di} \quad -f_{qi} \quad k_i^{-1} f_{mi} + k_i^{-1} \tau_{disi}]^T. \end{array} \right. \quad (7)$$

式(6)的哈密顿函数选择为

$$H(\mathbf{x}_i) = \frac{1}{2} \left(\frac{1}{L_{di}} x_{1i}^2 + \frac{1}{L_{qi}} x_{2i}^2 + \frac{1}{k_i^{-1} \bar{M}_{ii}} x_{4i}^2 \right) + k_i^{-1} \tau'_{Li} x_{3i}. \quad (8)$$

则式(6)的端口受控耗散哈密顿结构为

$$\left\{ \begin{array}{l} \dot{\mathbf{x}}_i = [\mathbf{J}(\mathbf{x}_i) - \mathbf{R}] \frac{\partial H(\mathbf{x}_i)}{\partial \mathbf{x}_i} + \mathbf{g} \mathbf{u}_i + \mathbf{g}_i \mathbf{f}_i; \\ \mathbf{y}_i = \mathbf{g}^T \frac{\partial H(\mathbf{x}_i)}{\partial \mathbf{x}_i}. \end{array} \right. \quad (9)$$

式中: $\mathbf{J}(\mathbf{x}_i)$ 为互联矩阵; \mathbf{R} 为阻尼矩阵; \mathbf{g}, \mathbf{g}_1 分别为控制输入和扰动输入矩阵,分别为

$$\mathbf{J}(\mathbf{x}_i) = \begin{bmatrix} 0 & 0 & 0 & j_{14i} \\ 0 & 0 & 0 & -j_{24i} \\ 0 & 0 & 0 & 1 \\ -j_{14i} & j_{24i} & -1 & 0 \end{bmatrix},$$

$$\mathbf{R} = \begin{bmatrix} R_i & 0 & 0 & 0 \\ 0 & R_i & 0 & 0 \\ 0 & 0 & 0 & 0 \\ 0 & 0 & 0 & k_i^{-1} \bar{C}_{ii} \end{bmatrix},$$

$$\mathbf{g} = \begin{bmatrix} 1 & 0 \\ 0 & 1 \\ 0 & 0 \\ 0 & 0 \end{bmatrix}, \mathbf{g}_1 = \begin{bmatrix} 1 & 0 & 0 \\ 0 & 1 & 0 \\ 0 & 0 & 0 \\ 0 & 0 & 1 \end{bmatrix}.$$

式中: $j_{14i} = n_p L_{qi} I_{qi} k_i^{-1}$, $j_{24i} = n_p (L_{di} I_{di} k_i^{-1} + \phi_i k_i^{-1})$ 。

2 控制系统设计

本文目标是通过设计鲁棒控制器来实现带有不确定性的PMSM驱动机械臂系统的末端位置高精度跟踪。位置跟踪的核心在于电流的准确跟踪。本文的思路是先设计级联ESO位置控制器得到期望电流 I_{qi}^* ,然后设计鲁棒IDA控制器来实现关节位置、电机电流跟踪,并改善初始控制输入大的问题。

2.1 级联ESO位置控制器设计

根据式(6)中的机械方程,定义新的控制输入 I_{qi}^* ,整理可得

$$\ddot{q}_i = b_{mi} I_{qi}^* + F_{mi}. \quad (10)$$

式中: $b_{mi} = n_p [\phi_i + (L_{di} - L_{qi}) I_{di}] / \bar{M}_{ii}$; F_{mi} 为机械子系统的总扰动,表示为

$$F_{mi} = b_{mi} (I_{qi} - I_{qi}^*) - \frac{\bar{C}_{ii}}{\bar{M}_{ii}} \dot{Q}_i + \frac{1}{\bar{M}_{ii}} (-\tau'_{Li} + f_{mi} + \tau_{disi}). \quad (11)$$

式(10)状态向量和输入向量定义为

$$\begin{cases} \mathbf{z}_i = [Q_i \quad \dot{Q}_i \quad F_{mi}]^T; \\ \mathbf{u}_{mi} = [I_{qi}^*] \end{cases} \quad (12)$$

式(10)的扩张状态空间模型为

$$\begin{cases} \dot{z}_{1i} = z_{2i}; \\ \dot{z}_{2i} = z_{3i} + b_{mi} I_{qi}^*; \\ \dot{z}_{3i} = \dot{F}_{mi} \end{cases} \quad (13)$$

$$\begin{cases} \dot{\hat{z}}_{1i} = \hat{z}_{2i} - \beta_{1i} (\hat{z}_{1i} - z_{1i}); \\ \dot{\hat{z}}_{2i} = \hat{z}_{3i} + b_{mi} I_{qi}^* - \beta_{2i} (\hat{z}_{1i} - z_{1i}); \\ \dot{\hat{z}}_{3i} = -\beta_{3i} (\hat{z}_{1i} - z_{1i}) \end{cases} \quad (14)$$

式中: \hat{z}_i 为对状态 z_i 的重构; $\beta_{1i}, \beta_{2i}, \beta_{3i}$ 为观测器增益; \hat{z}_{3i} 由于控制增益相关的不确定性也归到了总扰动中,因此不是对总扰动 F_{mi} 的完全估计。

第2个ESO的状态定义为 $s_i = [s_{1i} \ s_{2i} \ s_{3i}]^T$, s_{1i} 和 s_{2i} 分别追踪 z_{1i} 和 z_{2i} , $s_{3i} = F_{mi} - \hat{z}_{3i}$ 表示剩余的扰动误差,利用第1个ESO估计的 \hat{z}_{3i} ,第2个ESO设计为

$$\begin{cases} \dot{s}_{1i} = s_{2i} - \alpha_{1i} (\hat{s}_{1i} - z_{1i}); \\ \dot{s}_{2i} = s_{3i} + \hat{z}_{3i} + b_{mi} I_{qi}^* - \alpha_{2i} (\hat{s}_{1i} - z_{1i}); \\ \dot{s}_{3i} = -\alpha_{3i} (\hat{s}_{1i} - z_{1i}) \end{cases} \quad (15)$$

式中: $\alpha_{1i}, \alpha_{2i}, \alpha_{3i}$ 为观测器增益。

根据极点配置,两个ESO的观测器增益可选择为

$$\begin{cases} \beta_{1i} = 3\omega_0; \\ \beta_{2i} = 3\omega_0^2; \\ \beta_{3i} = \omega_0^3; \\ \alpha_{1i} = 3\omega_1; \\ \alpha_{2i} = 3\omega_1^2; \\ \alpha_{3i} = \omega_1^3. \end{cases} \quad (16)$$

综合 \hat{z}_{3i} 和 \hat{s}_{3i} ,控制律设计为

$$I_{qi}^* = (\ddot{Q}_{ides} + K_{pi} (Q_{ides} - \hat{z}_{1i}) + K_{di} (\dot{Q}_{ides} - \hat{z}_{2i}) - \hat{z}_{3i} - \hat{s}_{3i}) / b_{mi} \quad (17)$$

式中: $K_{pi} > 0, K_{di} > 0, K_{pi}, K_{di}$ 分别为比例增益和微分增益;由于期望的轨迹是光滑可导的,所以 $\ddot{Q}_{ides}, \dot{Q}_{ides}$ 是可知的。

2.2 鲁棒IDA控制器设计

平衡点 $\mathbf{x}_i^* = [L_{di} I_{di}^* \ L_{qi} I_{qi}^* \ Q_{ides} \ k_i^{-1} \bar{M}_{ii} \dot{Q}_{ides}]^T$ 得到后,针对式(9),令 $\mathbf{u}_i = \mathbf{u}_{li} + \mathbf{u}_{zi}$,其中 \mathbf{u}_{li} 为没有扰动时的IDA控制器, \mathbf{u}_{zi} 为针对扰动的 H_∞ 控制器。

当不考虑扰动时,期望的哈密顿函数选择为

$$H_{des}(\tilde{\mathbf{x}}_i) = \frac{1}{2} \left(\frac{1}{L_{di}} \tilde{x}_{1i}^2 + \frac{1}{L_{qi}} \tilde{x}_{2i}^2 + \frac{1}{k_i^{-1} \bar{M}_{ii}} \tilde{x}_{3i}^2 \right) + \frac{1}{2} \tilde{x}_{3i}^2 \quad (18)$$

状态误差定义为 $\tilde{\mathbf{x}}_i = \mathbf{x}_i - \mathbf{x}_i^*$,将 $\mathbf{x}_i = \tilde{\mathbf{x}}_i + \mathbf{x}_i^*$ 代入到式(9)可得

$$\dot{\tilde{\mathbf{x}}}_i = [\mathbf{J}(\tilde{\mathbf{x}}_i) + \bar{\mathbf{J}}(\mathbf{x}_i^*) - \mathbf{R}] \frac{\partial H(\tilde{\mathbf{x}}_i + \mathbf{x}_i^*)}{\partial (\tilde{\mathbf{x}}_i + \mathbf{x}_i^*)} +$$

$$\mathbf{g}(\mathbf{u}_{1i} + \mathbf{u}_{2i}) - \dot{\mathbf{x}}_i^* = 0 \quad (19)$$

式中:

$$\tilde{\mathbf{J}}(\mathbf{x}_i^*) = \begin{bmatrix} 0 & 0 & 0 & n_p x_{2i}^* k_i^{-1} \\ 0 & 0 & 0 & -n_p x_{1i}^* k_i^{-1} \\ 0 & 0 & 0 & 0 \\ -n_p x_{2i}^* k_i^{-1} & n_p x_{1i}^* k_i^{-1} & 0 & 0 \end{bmatrix};$$

$$\dot{\mathbf{x}}_i^* = [\mathbf{J}(\mathbf{x}_i^*) - \mathbf{R}] \frac{\partial H(\mathbf{x}_i^*)}{\partial \mathbf{x}_i^*} + \mathbf{g}\mathbf{u}_{i0};$$

$$\mathbf{u}_{i0} = \begin{bmatrix} -n_p L_{qi} I_{qi}^* k_i^{-1} \dot{Q}_{ides} \\ L_{qi} \frac{dI_{qi}^*}{dt} + R_i I_{qi}^* + n_p \phi_i k_i^{-1} \dot{Q}_{ides} \end{bmatrix}.$$

期望的状态误差闭环哈密顿结构设计为

$$\dot{\tilde{\mathbf{x}}}_i = [\mathbf{J}_{des}(\tilde{\mathbf{x}}_i) - \mathbf{R}_{des}] \frac{\partial H_{des}(\tilde{\mathbf{x}}_i)}{\partial \tilde{\mathbf{x}}_i} + \mathbf{g}\mathbf{u}_{2i}. \quad (20)$$

式中: $\mathbf{J}_{des}(\tilde{\mathbf{x}}_i)$ 为期望的互联矩阵; \mathbf{R}_{des} 为期望的耗散矩阵。 $\mathbf{J}_{des}(\tilde{\mathbf{x}}_i) = \mathbf{J}(\tilde{\mathbf{x}}_i) + \mathbf{J}_a$, \mathbf{J}_a 为注入的互联矩阵, $\mathbf{R}_{des} = \mathbf{R} + \mathbf{R}_a$, \mathbf{R}_a 为注入的耗散矩阵, 分别表示为

$$\mathbf{J}_a = \begin{bmatrix} 0 & J_{12i} & J_{13i} & J_{14i} \\ -J_{12i} & 0 & J_{23i} & J_{24i} \\ -J_{13i} & -J_{23i} & 0 & J_{34i} \\ -J_{14i} & -J_{24i} & -J_{34i} & 0 \end{bmatrix},$$

$$\mathbf{R}_a = \begin{bmatrix} r_{1i} & 0 & 0 & 0 \\ 0 & r_{2i} & 0 & 0 \\ 0 & 0 & 0 & 0 \\ 0 & 0 & 0 & 0 \end{bmatrix}.$$

令式(19)和式(20)相等, 计算可得 \mathbf{u}_{1i} 为

$$\begin{cases} u_{1di} = -r_{1i} I_{di} + J_{12i} \tilde{I}_{qi} - n_p L_{qi} k_i^{-1} I_{qi} \dot{Q}_i; \\ u_{1qi} = -J_{12i} I_{di} - r_{2i} \tilde{I}_{qi} + R_i I_{qi}^* + n_p L_{di} I_{di} k_i^{-1} \dot{Q}_i + n_p \phi_i k_i^{-1} \dot{Q}_i^* + L_{qi} \frac{dI_{qi}^*}{dt}. \end{cases} \quad (21)$$

考虑扰动, 式(21)代入到式(9)可得

$$\begin{cases} \dot{\tilde{\mathbf{x}}}_i = [\mathbf{J}_{des}(\tilde{\mathbf{x}}_i) - \mathbf{R}_{des}] \frac{\partial H_{des}(\tilde{\mathbf{x}}_i)}{\partial \tilde{\mathbf{x}}_i} + \mathbf{g}\mathbf{u}_{2i} + \mathbf{g}\mathbf{f}_i; \\ \tilde{\mathbf{y}}_i = \mathbf{g}^T \frac{\partial H_{des}(\tilde{\mathbf{x}}_i)}{\partial \tilde{\mathbf{x}}_i}. \end{cases} \quad (22)$$

式(22)的 H_∞ 控制问题^[3] 可描述为: 设计 \mathbf{u}_{2i} , 使得哈密顿-雅克比不等式恒成立, 即

$$\begin{aligned} & \left[\frac{\partial H_{des}(\tilde{\mathbf{x}}_i)}{\partial \tilde{\mathbf{x}}_i} \right]^T \{ [\mathbf{J}_{des}(\tilde{\mathbf{x}}_i) - \mathbf{R}_{des}] \left[\frac{\partial H_{des}(\tilde{\mathbf{x}}_i)}{\partial \tilde{\mathbf{x}}_i} \right] + \mathbf{g}\mathbf{u}_{2i} \} + \frac{1}{2\gamma^2} \left[\frac{\partial H_{des}(\tilde{\mathbf{x}}_i)}{\partial \tilde{\mathbf{x}}_i} \right]^T \mathbf{g}\mathbf{g}^T \left[\frac{\partial H_{des}(\tilde{\mathbf{x}}_i)}{\partial \tilde{\mathbf{x}}_i} \right] \\ & \frac{1}{2} \left[\frac{\partial H_{des}(\tilde{\mathbf{x}}_i)}{\partial \tilde{\mathbf{x}}_i} \right]^T \mathbf{g}\mathbf{g}^T \left[\frac{\partial H_{des}(\tilde{\mathbf{x}}_i)}{\partial \tilde{\mathbf{x}}_i} \right] \leq 0. \end{aligned} \quad (23)$$

则 \mathbf{f}_i 到 $\tilde{\mathbf{y}}_i$ 的 L_2 增益小于给定的扰动抑制水平 γ , 即

$$\int_0^T \| \tilde{\mathbf{y}}_i \|^2 dt \leq \gamma^2 \int_0^T \| \mathbf{f}_i \|^2 dt. \quad (24)$$

根据式(23), 如果 $\mathbf{R}_{des} + \frac{1}{2\gamma^2} (\mathbf{g}\mathbf{g}^T - \mathbf{g}_1\mathbf{g}_1^T)$ 正定, 则 H_∞ 控制律可选择为

$$\mathbf{u}_{2i} = -\frac{1}{2} \left(1 + \frac{1}{\gamma^2} \right) \mathbf{g}^T \frac{\partial H_{des}(\tilde{\mathbf{x}}_i)}{\partial \tilde{\mathbf{x}}_i}. \quad (25)$$

因此鲁棒 IDA 控制器为

$$\begin{cases} u_{di} = -r_{1i} I_{di} + J_{12i} \tilde{I}_{qi} - n_p L_{qi} k_i^{-1} I_{qi} \dot{Q}_i - \frac{1}{2} \left(1 + \frac{1}{\gamma^2} \right) I_{di}; \\ u_{qi} = -J_{12i} I_{di} - r_{2i} \tilde{I}_{qi} + R_i I_{qi}^* + n_p L_{di} I_{di} k_i^{-1} \dot{Q}_i + n_p \phi_i k_i^{-1} \dot{Q}_i^* + L_{qi} \frac{dI_{qi}^*}{dt} - \frac{1}{2} \left(1 + \frac{1}{\gamma^2} \right) \tilde{I}_{qi}. \end{cases} \quad (26)$$

2.3 改进的鲁棒 IDA 控制器设计

由式(26)可知, 在 IDA 上加入 H_∞ 控制电流

误差 \tilde{I}_{qi} 的比例增益从 r_{2i} 增大到 $r_{2i} + 0.5(1+1/\gamma^2)$ 。考虑到开始时电流误差 \tilde{I}_{qi} 很大, 如果直接引入 H_∞ 控制, 会导致初始控制输入特别大。为了改善初始控制输入大的问题, 依据大误差小增益、小误差大增益的原则改进了 H_∞ 控制引入的时机。即电流误差绝对值过大时只采用 IDA 控制, 这样即使开始时电流误差大, 由于给定的增益小, 初始控制电压也不会很大; 电流误差绝对值小于设定值时, 再在 IDA 上引入 H_∞ 控制, 这样改进的鲁棒 IDA 控制器为

$$\begin{cases} \mathbf{u}_i = \mathbf{u}_{1i}, |I_{qi}^* - I_{qi}| > \varepsilon_i; \\ \mathbf{u}_i = \mathbf{u}_{1i} + \mathbf{u}_{2i}, 0 \leq |I_{qi}^* - I_{qi}| < \varepsilon_i. \end{cases} \quad (27)$$

式中: $\varepsilon_i > 0$ 为变增益所选择的设定值。

3 稳定性分析

本文的控制结构是先设计级联 ESO 位置控制器得到 I_{qi}^* , 然后设计改进的鲁棒 IDA 控制器实现位置、电流的高精度鲁棒跟踪。因此整体系统的稳定性需要先保证 I_{qi}^* 能使关节位置实现渐近跟踪, 然后在整体系统没有扰动时证明 IDA 控制的渐近稳定, 最后在扰动存在时保证从扰动 f_i 到输出 \tilde{y}_i 的 L_2 增益小于给定的扰动抑制水平 γ 。

位置跟踪误差定义为 $e_{si} = Q_i - Q_{ides}$, 将式(17)代入到式(10), 整理可得

$$\ddot{e}_{si} = -K_{pi}e_{si} - K_{di}\dot{e}_{si} - K_{pi}\tilde{z}_{li} - K_{di}\tilde{z}_{2i} - \tilde{s}_{3i}。 \quad (28)$$

式中: $\tilde{z}_i = \hat{z}_i - z_i$ 、 $\tilde{s}_i = \hat{s}_i - s_i$ 均为观测器误差。

令 $X_{ei} = [e_{si} \ \dot{e}_{si} \ \tilde{z}_{1i} \ \tilde{z}_{2i} \ \tilde{s}_{3i}]^T$, 根据两个观测器的误差系统, 则式(28)的状态空间表达式为

$$\dot{X}_{ei} = \begin{bmatrix} 0 & 1 & 0 & 0 & 0 \\ -K_{pi} & -K_{di} & -K_{pi} & -K_{di} & -1 \\ 0 & 0 & -\beta_{li} & 1 & 0 \\ 0 & 0 & -\beta_{2i} & 0 & 1 \\ 0 & 0 & -\alpha_{3i} & 0 & 0 \end{bmatrix} X_{ei}。 \quad (29)$$

根据计算, 式(29)系统矩阵的特征值小于 0, 因此式(29)系统是渐近稳定的。根据极点配置, 比例、积分增益分别为 $K_{pi} = \omega_c^2$, $K_{di} = 2\omega_c$, ω_c 为闭环系统带宽。

不考虑扰动时, 控制律为 $u_i = u_{1i}$, 闭环系统的李雅普诺夫函数设计为 $V_i = H_{des}(\tilde{x}_i)$, 其导数为

$$\dot{V}_i = \left[\frac{\partial H_{des}(\tilde{x}_i)}{\partial \tilde{x}_i} \right]^T \dot{\tilde{x}}_i = - \left[\frac{\partial H_{des}(\tilde{x}_i)}{\partial \tilde{x}_i} \right]^T。 \\ R_{des} \frac{\partial H_{des}(\tilde{x}_i)}{\partial \tilde{x}_i} \leq 0。 \quad (30)$$

$$\text{若 } \tilde{x}_i = \mathbf{0}, \text{ 则 } \frac{\partial H_{des}(\tilde{x}_i)}{\partial \tilde{x}_i} = \mathbf{0}, \frac{\partial^2 H_{des}(\tilde{x}_i)}{\partial \tilde{x}_i^2} \geq 0$$

0。根据 LaSalle 不变集原理, 如果集合 $\{\tilde{x}_i = \mathbf{0}\}$

是包含在集合 $\left\{ \tilde{x}_i \in \mathbb{R}^4 \mid \left[\frac{\partial H_{des}(\tilde{x}_i)}{\partial \tilde{x}_i} \right]^T R_{des} \cdot \frac{\partial H_{des}(\tilde{x}_i)}{\partial \tilde{x}_i} = 0 \right\}$ 内的最大不变集, 则式(9)系统

在平衡点 x_i^* 处是渐近稳定的。

考虑扰动, 当引入 H_∞ 时, $u_i = u_{1i} + u_{2i}$, 能使式(23)成立, 因此从 f_i 到输出 \tilde{y}_i 的 L_2 增益小于 γ 。

4 仿真验证

利用 MATLAB/Simulink 搭建仿真系统, 以 2 个 PMSM 驱动两关节系统为例进行仿真验证。本文采用文献[5]使用的机械臂模型和参数值, $F_1 = 0.1\dot{Q}_1, F_2 = 0.1\dot{Q}_2$ 。电机参数为 $R_1 = R_2 = 0.338 \Omega, L_{d1} = L_{d2} = L_{q1} = L_{q2} = 1.515 \times 10^{-3} \text{ H}, n_p = 4, \phi_{f1} = \phi_{f2} = 0.07287 \text{ Wb}, J_1 = J_2 = 0.00111 \text{ kg} \cdot \text{m}^3, r_1 = r_2 = 0.01$ 。初始位置、速度均为 0, 期望轨迹为 $Q_{1des} = 0.1\sin 3t + 0.5\cos 3t, Q_{2des} = 0.1\sin 4t + 0.5\cos 4t, \tau_{ext} = [30\sin 3t \ 30\sin 3t]^T$, 系统参数在 50% 内变化。第 i 个 PMSM 驱动第 i 个关节的仿真结构如图 1 所示, 图 1 中的 $u_{ai}, u_{bi}, I_{ai}, I_{bi}$ 分别为 $\alpha\beta$ 坐标系下的电压和电流, $u_{ai}, u_{bi}, u_{ci}, I_{ai}, I_{bi}, I_{ci}$ 分别为 abc 坐标系下的电压和电流。

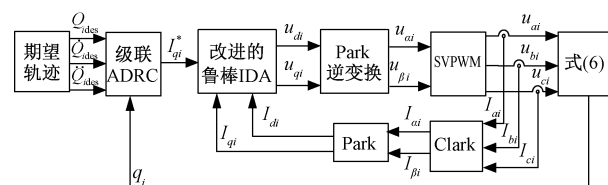


图 1 电驱动机械臂系统的控制结构图

Figure 1 Control structure diagram of electrically driven manipulator system

首先, 在依据机械子系统方程得到 I_{qi}^* 的过程中, 先对级联 ESO 与传统 ESO 比较, 控制器参数选择为 $K_{P1} = K_{P2} = 100, K_{D1} = K_{D2} = 20, \omega_0 = 100, \omega_1 = 300, r_1 = r_2 = 1, j_{2i} = 0, \gamma = 0.1$ 。关节位置跟踪误差对比如图 2 所示。可以看出, 由于传统 ESO 估计的总扰动有误差, 因此传统 ESO 的关节位置跟踪精度相对较低, 而级联 ESO 估计了机械子系统的剩余总扰动, 位置跟踪精度更高。级联 ESO 与传统 ESO 相比位置跟踪精度提升了 0.003 rad。

其次, 对改进的鲁棒 IDA 控制与 IDA 控制进行比较, 关节位置跟踪和电流跟踪对比如图 3 和图 4 所示。可以看出, 即使采用了级联 ESO, IDA 控制的位置跟踪精度仍相对较低, 说明即使机械子系统有很强的鲁棒性, 电气子系统的不确定性仍能影响到位置跟踪性能; 而改进的鲁棒 IDA 控制有效抑制了电气子系统的不确定性, 从而保证了位置、电流的高精度跟踪精度。改进的鲁棒控制器与哈密顿控制器相比, 关节位置跟踪精度提

升了 0.005 rad , 电流跟踪精度也显著提升。

再次, 将改进的鲁棒 IDA 控制与鲁棒 IDA 控制进行控制电压对比, 如图 5 所示。可以看出, 直接在 IDA 上引入 H_∞ , 初始控制电压特别大; 若改进 H_∞ 引入的时机, 可以极大地改善初始控制电压大的问题。

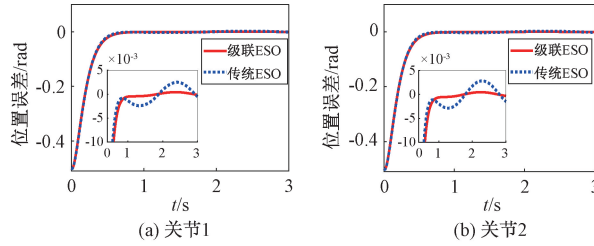


图 2 级联 ESO 与传统 ESO 的位置跟踪误差对比

Figure 2 Position tracking error comparison between cascaded ESO and traditional ESO

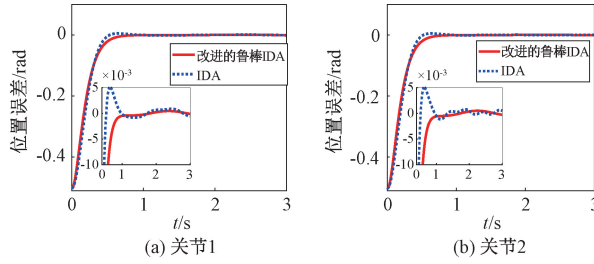


图 3 改进的鲁棒 IDA 与 IDA 的位置跟踪误差对比

Figure 3 Position tracking error comparison between improved robust IDA and IDA

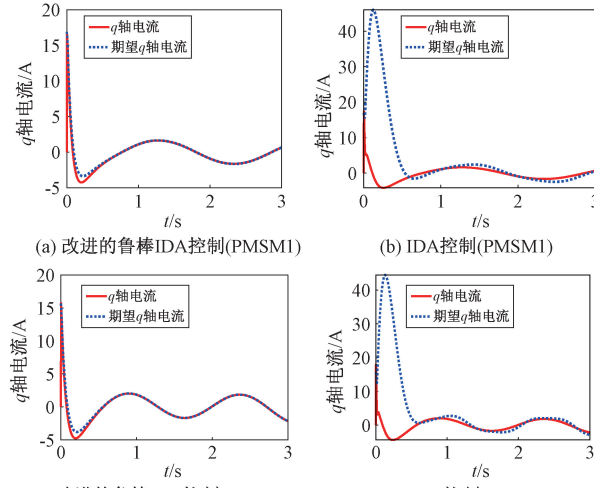


图 4 改进的鲁棒 IDA 与 IDA 的电流跟踪误差对比

Figure 4 Current tracking error comparison between improved robust IDA and IDA

最后, 将本文提出的控制算法与 ADRC 控制器^[12]进行关节位置跟踪, 误差对比如图 6 所示。可以看出, 本文提出的控制算法具有更高的位置跟踪精度。本文采用的级联 ESO 位置控制器在机械、电气不确定性存在的情况下能准确地计算出 I_{qi}^* 。

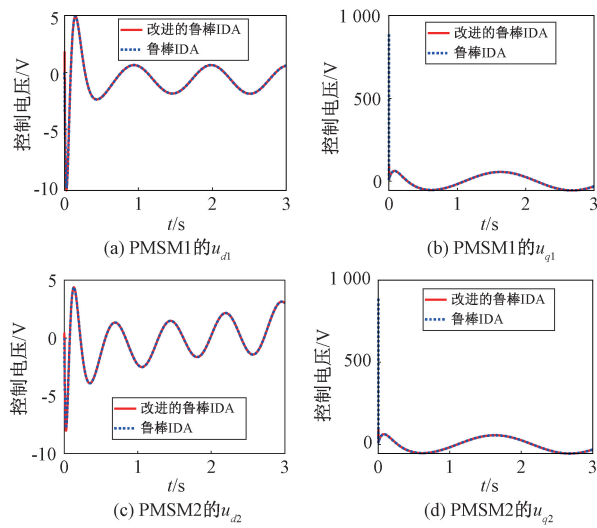


图 5 改进的鲁棒 IDA 与鲁棒 IDA 的电压对比

Figure 5 Voltage comparison between improved robust IDA and robust IDA

IDA and robust IDA

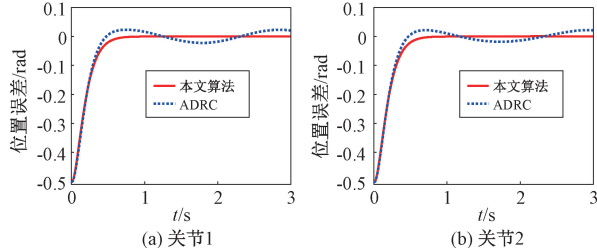


图 6 本文算法与电驱动 ADRC 的位置跟踪误差对比

Figure 6 Position tracking error comparison between proposed controller and electric driven ADRC control

5 结论

针对带有不确定性的 PMSM 驱动刚性机械臂的轨迹跟踪问题, 提出了自抗扰控制与鲁棒哈密顿控制相结合的控制策略。通过级联 ESO 位置控制器补偿机械子系统剩余总扰动, 从而提升关节位置跟踪精度, 并得到了 I_{qi}^* 。系统平衡点得到后, 设计 IDA 与 H_∞ 结合的鲁棒哈密顿控制器保证位置和电流的鲁棒跟踪, 同时改进了 H_∞ 控制引入的时机, 改善了初始控制输入过大的问题。本文设计的控制算法无须速度测量, 计算量小、静态精度高、鲁棒性强。在未来的研究中, 将考虑测量噪声的抑制问题, 并将学习算法用于控制增益的调节。

参考文献:

- [1] VERASTEGUI-GALVÁN J, HERNÁNDEZ-GUZMÁN V M, ORRANTE-SAKANASSI J. PID position regulation in one-degree-of-freedom Euler-Lagrange systems actuated by a PMSM [J]. International journal of con-

- trol, 2018, 91(2): 285–296.
- [2] UDDIN M N, ZHAI Z Q, AMIN I K. Port controlled Hamilton with dissipation-based speed control of IPMSM drive [J]. IEEE transactions on power electronics, 2020, 35(2): 1742–1752.
- [3] WU Z Q, WU C H, JIA W J, et al. Sensorless speed H_∞ control for PMSM based on energy function [J]. Optimal control applications and methods, 2017, 38(6): 949–955.
- [4] 张震, 沈学珂, 程欣. 永磁同步电机全速范围内无位置传感器控制 [J]. 郑州大学学报(工学版), 2019, 40(2): 35–40.
ZHANG Z, SHEN X K, CHENG X. Sensorless control of permanent magnet synchronous motor in full speed range [J]. Journal of Zhengzhou university (engineering science), 2019, 40(2): 35–40.
- [5] SUN W W, WU Y, WANG L P. Trajectory tracking of constrained robotic systems via a hybrid control strategy [J]. Neurocomputing, 2019, 330: 188–195.
- [6] ALI M, ALEXANDER C K. Trajectory tracking control for a robotic manipulator using nonlinear active disturbance rejection control [C]//ASME 2017 Dynamic Systems and Control Conference. New York: ASME, 2017: 1–8.
- [7] HAN Y, LI H, LI W T. Research on PMSM sensorless system based on ADRC-PBC strategy [C]//2016 Chinese Control and Decision Conference (CCDC). Piscataway: IEEE, 2016: 3186–3191.
- [8] 徐旭, 于海生, 于金鹏, 等. 永磁同步电机驱动的机器人哈密顿与PD协调控制 [J]. 制造业自动化, 2018, 40(10): 42–47.
XU X, YU H S, YU J P, et al. Robot joint driven by permanent magnet synchronous motor position control based on port-controlled Hamiltonian and PD coordination control method [J]. Manufacturing automation, 2018, 40(10): 42–47.
- [9] XUE Y, YU H S, LIU X D. Improved fuzzy backstepping position tracking control for manipulator driven by PMSM [C]//2018 Chinese Automation Congress (CAC). Piscataway: IEEE, 2018: 3561–3565.
- [10] KHORASHADIZADEH S, SADEGHIALEH M. Adaptive fuzzy tracking control of robot manipulators actuated by permanent magnet synchronous motors [J]. Computers & electrical engineering, 2018, 72: 100–111.
- [11] KEIGHOBADI J, FATEH M M. Adaptive robust tracking control based on backstepping method for uncertain robotic manipulators including motor dynamics [J]. International journal of industrial electronics, control and optimization, 2021, 4(1): 13–22.
- [12] SALEKI A, FATEH M M. Model-free control of electrically driven robot manipulators using an extended state observer [J]. Computers & electrical engineering, 2020, 87: 106768.
- [13] ORTEGA R, Var Der SCHAFT A, MASCHKE B, et al. Interconnection and damping assignment passivity-based control of port-controlled Hamiltonian systems [J]. Automatica, 2002, 38(4): 585–596.
- [14] HAN J Q. From PID to active disturbance rejection control [J]. IEEE transactions on industrial electronics, 2009, 56(3): 900–906.
- [15] 金宇治, 李光一, 刘金凤, 等. 内置式永磁同步电机自抗扰-无源控制策略 [J]. 电机与控制学报, 2020, 24(12): 35–42.
JIN N Z, LI G Y, LIU J F, et al. IPMSM control system based on ADRC-PBC strategy [J]. Electric machines and control, 2020, 24(12): 35–42.
- [16] ALONGE F, CIRRINCIONE M, D'IPPOLITO F, et al. Robust active disturbance rejection control of induction motor systems based on additional sliding-mode component [J]. IEEE transactions on industrial electronics, 2017, 64(7): 5608–5621.
- [17] DONG Q R, LIU Y K, ZHANG Y L, et al. Improved ADRC with ILC control of a CCD-based tracking loop for fast steering mirror system [J]. IEEE photonics journal, 2018, 10(4): 1–14.
- [18] WANG G L, LIU R, ZHAO N N, et al. Enhanced linear ADRC strategy for HF pulse voltage signal injection-based sensorless IPMSM drives [J]. IEEE transactions on power electronics, 2019, 34(1): 514–525.
- [19] 赵庆岩, 黎杰, 吴顺, 等. 基于遗传算法优化的机械臂动态矩阵预测控制 [J]. 郑州大学学报(工学版), 2020, 41(1): 32–37.
ZHAO Q Y, LI J, WU S, et al. Dynamic matrix predictive control of manipulators based on genetic algorithms [J]. Journal of Zhengzhou university (engineering science), 2020, 41(1): 32–37.

(下转第 15 页)

based on the human pose estimation technology, the dynamic characteristic parameters of standing stake process were extracted, and the digital expression and evaluation system of standing stake posture was constructed. Firstly, the human pose estimation algorithm OpenPose was used to extract the human keypoints from the video of standing stake. Secondly, the key characteristic parameters of digital expression were determined according to the essentials of standing stake. Then, the dynamic time warping algorithm and discriminant analysis method were used to calculate the evaluation indexes of each characteristic parameter. Finally, based on the long-term standing stake data, the coefficient of variation method was used to assign different weights to each evaluation index, to discuss the importance of each characteristic parameter and to comprehensively evaluate standing stake performance. The specific implementation included: designing an experiment to collect standing stake video from the front and side, six Tai Chi professional experts and twenty-two students participated in this research, and the students were divided into experimental and control groups. Through the analysis of standing stake parameters of the expert group, it was found that standing stake was actually a dynamic process, and the experimental data expressed the dynamic characteristic parameters of different parts from the front and side. At the same time, the long-term standing stake data of students in the experimental group was tracked for eight months. Through the comparative evaluation with the expert data, it revealed that the trunk, thigh, knee and hip were the more important body parts in standing stake process. In addition, after digital evaluation and guidance, standing stake quality of students in the experimental group was significantly improved, which could verify the effectiveness of digital expression and evaluation system for auxiliary training.

Keywords: standing stake; OpenPose; characteristic parameters; evaluation index; auxiliary training

(上接第7页)

Active Disturbance Rejection Robust Hamiltonian Tracking Control of Electrically Driven Manipulator

ZENG Qingshan, ZHOU Yashuai, TAO Changchun, LIU Yanhong

(School of Electrical Engineering, Zhengzhou University, Zhengzhou 450001, China)

Abstract: Aiming to solve the position tracking problem of permanent magnet synchronous motor driven manipulator system, a robust control strategy combining active disturbance rejection control and Hamiltonian control was proposed. Firstly, the electrical subsystem and mechanical subsystem model considering uncertainty were established, and the model was transformed into a single-motor-driven single-joint port Hamiltonian structure according to the independent joint control idea. Then, the cascaded extended state observer was designed to estimate the total disturbance of the mechanical subsystem, and the designed control law achieved robust tracking of the desired position while simply and efficiently obtaining the desired q -axis current. Finally, a robust Hamiltonian controller which could combine the interconnections and damping assignment Hamiltonian controller with the H_∞ controller based on the system Hamiltonian structure was designed to achieve high precision robust current tracking, and improves the problem of large initial control input by improving the timing of introducing H_∞ . Compared with modelless active disturbance rejection control of the electrically driven robot manipulators, the simulation results verified the effectiveness of the proposed control scheme. Compared with traditional ESO, the joint position tracking accuracy of the cascaded ESO could be improved by 0.003 rad. Compared with the Hamiltonian controller, the joint position tracking accuracy of the improved robust Hamiltonian controller was improved by 0.005 rad, the current tracking accuracy was significantly improved, and the initial control input of the improved H_∞ introduction timing was significantly reduced.

Keywords: electrically driven manipulator; tracking control; port Hamilton system; active disturbance rejection control; robust control